DOI 10.1007/s10891-015-1177-7
Journal of Engineering Physics and Thermophysics, Vol. 88, No. 1, January, 2015

MEASUREMENT OF THE THERMAL-CONDUCTIVITY COEFFICIENT OF NANOFLUIDS BY THE HOT-WIRE METHOD

A.V. Minakov,[a,b] V. Ya. Rudyak,[c] D. V. Guzei,[a] M. I. Pryazhnikov,[a] and A. S. Lobasov[a,b]

UDC 536.2,53.082

In this work, the authors present results of adaptation and testing of the hot-wire method for determination for the thermal-conductivity coefficient of nanofluids. A mathematical model of heat transfer with allowance for free convection has been constructed to elucidate the parameters of an experimental setup and the range of its applicability. The experimental procedure has been tested on measurements of the thermal conductivities of water and ethylene glycol. The thermal-conductivity coefficient of a nanofluid has been measured at room temperature. The nanofluid under study was prepared on the basis of ethylene glycol and alumina nanoparticles. The concentrations of the nanoparticles ranged from 0.5% to 2% by volume. Good agreement has been obtained between the measured values of the thermal-conductivity coefficient and the data of other authors.

Keywords: *heat conduction, hot-wire method, free convection, nanoparticles, nanofluid, CFD (computational fluid dynamics), experiment.*

Introduction. The first use of a fluid with microparticles for the purpose of heat-transfer intensification has been known since the mid-1970s (e.g., Ahuja, 1975 [1]). However, it failed to obtain substantial results. This is due to the fact that large disperse particles sediment quite rapidly and cause the channel walls to erode. Fluids in which the dispersed component is represented by nanoparticles are free from this drawback. The idea of using nanoparticles to enhance the heat conduction of a carrier fluid emerged about two decades ago. A two-phase medium whose carrier component is a regular liquid and whose dispersed component is represented by nanoparticles is currently referred to as a nanofluid (this term appeared for the first time in the work of Choi [2]). At present, one important fundamental issue is understanding mechanisms of transfer of heat in nanofluids. To explain the anomalous heat conduction of nanofluids one analyzes a few mechanisms: Brownian motion of nanoparticles (diffusion), the formation of a high-thermal-conductivity liquid layer on the "liquid–particle" interface, classification of nanoparticles, thermal diffusion (transfer of nanoparticles by the action of a temperature gradient), ballistic transfer of thermal energy in an individual particle and between nanoparticles occurring in the case of their contact, and others. The issue as to the contribution of these mechanisms to the effective thermal conductivity of various nanofluids remains open. Due to this, no general theory capable of predicting reliably the heat conduction of nanofluids has been created to date. Therefore, a reliable experimental procedure of measurement of the thermal-conductivity coefficient of nanofluids is required.

Despite the great number of works in which the heat conduction of nanofluids and their heat transfer are studied, the results obtained are often erratic. This is true of, e.g., heat transfer under natural-convection conditions [3]. Although an enhancement of the heat transfer in the case where nanoparticles are used is noted in most works [4], there are publications where a decrease in the heat transfer on adding them is demonstrated [5]. In addition to experimental investigations of the heat conduction of nanofluids, there are numerous theoretical works; however, a review of results of works by different researchers shows that it is impossible to closely predict the heat conduction of nanofluids at present. Therefore, comprehensive investigations of the heat transfer of nanofluids require a reliable procedure of measurement of the thermal-conductivity coefficient.

The present work seeks to adapt and test an experimental procedure of determination of the thermal-conductivity coefficient of nanofluids that is based on the well-known hot-wire method [6–8]. This method is widely employed to measure

[a]Siberian Federal University, 79 Svobodnyi Ave., Krasnoyarsk, 660041, Russia; email: Aminakov@sfu-kras.ru; [b]S. S. Kutateladze Institute of Thermophysics, Siberian Branch of the Russian Academy of Sciences, 1 Akad. Lavrentiev Ave., Novosibirsk, 630090, Russia; [c]Novosibirsk State University of Architecture and Civil Engineering, 113 Leningradskaya Str., Novosibirsk, 630008, Russia. Translated from Inzhenerno-Fizicheskii Zhurnal, Vol. 88, No. 1, pp. 148–160, January–February, 2015. Original article submitted August 20, 2014.

the thermal-conductivity coefficient of liquids. The central problem in this case is that the accuracy of measurements can be influenced significantly by free convection. In most works, one uses the existing empirical dependences of convective heat transfer to evaluate the time of development of free convection. It is shown below that in many cases such evaluations cannot be considered reliable. However, for creation of an experimental setup and processing of experimental results, it is required that the range of applicability be determined. In our work, such evaluation is performed using computational-hydrodynamics and heat-transfer methods.

Theoretical Principles of the Hot-Wire Method. The hot-wire method for measurement of the thermal conductivity of gases was proposed by Schleiermacher [6] in 1888. Its detailed description can be found in [7, 8]. The modern digital hot-wire method has been described in [9, 10]. The principle of measurement of the thermal conductivity by the hot-wire method [6–10] is based on the linear dependence between the growth in the wire temperature and the logarithm of the heating time. In the homogeneous fluid under study, there is immersed a wire; a direct electric current is passed through the wire, and the heat flux on it is constant. For an ideal linear source, the basic process of propagation of heat around the wire is described by the Fourier equation

$$\frac{\partial T}{\partial t} = a\nabla^2 T \tag{1}$$

with the following boundary and initial conditions:

$$\Delta T\,(r, t) = 0 \quad (t \le 0, \text{ at any } r)\,,$$

$$\lim_{r\to 0}\left(r\,\frac{\partial T}{\partial t}\right) = -\frac{q}{2\pi\lambda}\,(r = 0,\ t \ge 0)\,,$$

$$\lim_{r\to\infty}\Delta T\,(r, t) = 0 \quad (r \to \infty,\ t \ge 0)\,,$$

where ΔT determines the growth in the temperature of the hot wire, a and λ are the thermal diffusivity and thermal conductivity of the fluid, and q is the constant heat flux released by the hot wire per unit length.

The solution of Eq. (1) is

$$\Delta T\,(r, t) = \frac{q}{4\pi\lambda}\,E_1\left(\frac{4at}{r^2}\right),$$

where

$$E_1\,(B) = \int_B^\infty\left(\frac{e^{-x}}{x}\right)dx \cong -\gamma - \ln B + B + o\left(B^2\right),$$

$$\gamma = \ln C, \quad B = \frac{r^2}{4at}, \quad C = 1.781\,.$$

When r is equal to the hot-wire radius r_w, which has a very small value (as B), the above solution can additionally be simplified. Finally, we obtain the following asymptotic solution:

$$\Delta T\,(r_w, t) = \left(\frac{q}{4\pi\lambda}\right)\ln\left(\frac{4at}{r_w^2 C}\right) = H\,\ln t + A\,. \tag{2}$$

Equation (2) expresses the linear dependence between ΔT and $\ln t$. The actual temperature distribution of the wire in the process of its heating is shown in Fig. 1. It is seen that there is a portion of the temperature curve on which the behavior of ΔT is nearly linear indeed. The presence of the intrinsic heat capacity in the wire leads to the fact that the actual distribution $\Delta T = f(\ln t)$ will differ from the linear dependence on the initial portion of the curve. The deviation of this dependence from the linear one at the final stage of heating is primarily due to the development of free convection. Thus, determining the

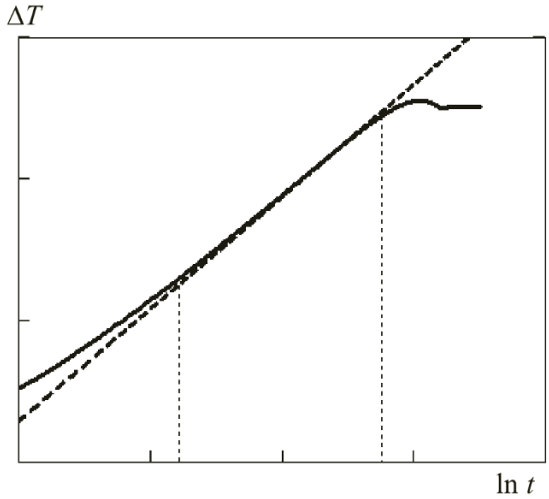

Fig. 1. Typical distribution of the wire temperature: solid curve, experimental values [14], dashed curve, asymptotic solution (2).

boundaries of the range of the linear dependence, we can determine the thermal conductivity of the fluid from the slope of the straight line $\Delta T \sim \ln t$ (H) and the linear heat-flux density using the following expression:

$$\lambda = \frac{q}{4\pi H} . \tag{3}$$

Mathematical Model and Modeling Results. As has already been stated, the central problem with the measurement of the thermal-conductivity coefficient of the fluid is that the measurements can be greatly influenced by free convection. For the experiment results to be interpreted correctly, one should be aware of the cases where this influence becomes substantial. Therefore, to describe and understand the essence of thermophysical processes occurring on the wire in its unsteady heating, we have constructed a two-dimensional mathematical model of heat transfer with allowance for free convection. In this model, the fluid is considered as a homogeneous incompressible Newtonian medium whose flow is described by the Navier–Stokes equations

$$\nabla(\rho \mathbf{v}) = 0 ,$$

$$\frac{\partial \rho \mathbf{v}}{\partial t} + \nabla(\rho \mathbf{v}\mathbf{v}) = -\nabla p + \nabla \mathbf{T} + \rho g ,$$

where ρ is the density of the fluid, p is the pressure, $\mathbf{v}$ is the velocity vector, and $\mathbf{T}$ is the viscous-stress tensor.

The energy equation is represented in the following form:

$$\frac{\partial \rho h}{\partial t} + \nabla \left(\rho v h\right) = \nabla \left(\lambda \nabla T\right) ,$$

where the medium′s enthalpy is determined as $h(T) = \int_{T_0}^{T} C_p dT$, and the density of the fluid, as $\rho = \frac{\rho_0}{1 + \beta(T - T_0)}$, where ρ_0 is the density of the fluid at the room temperature T_0, and β is the coefficient of thermal expansion of the fluid.

The problem was solved in a two-dimensional formulation. In the calculations, we considered versions with a vertical and a horizontal arrangement of the hot wire. For the horizontal arrangement, the computational domain represented a ring whose inside diameter was equal to a wire diameter of 75 μm. The outside diameter of the computational domain was equal to 6 cm. Methodological calculations have shown that this diameter of the computational domain does not influence the heat transfer on the wire.

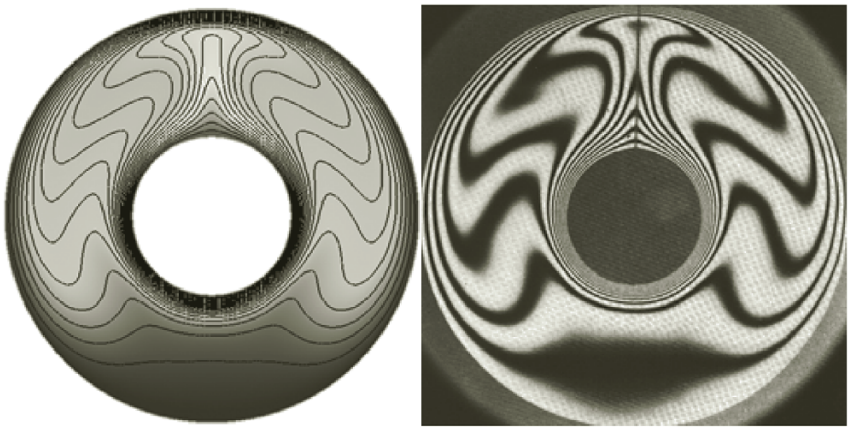

a *b*

Fig. 2. Temperature distribution in the space between cylinders: a) calculated isolines of temperature; b) experimental interferogram of the temperature field [15].

On the internal boundary of the computational domain, we prescribed a fixed heat-flux value equal to the experimental value of the heat flux on the wire. On the external boundary, we adopted the condition of the absence of the heat flux. Although this condition is not quite consistent with experimental conditions, it may be considered as fairly correct because of the short duration of the process and of the fact that the dimensions of the computational domain are many times larger than the diameter of the wire.

At the initial instant of time, the fluid temperature in the computational domain was prescribed to be uniform and equal to 25^{o}C. The medium was quiescent. The gravity force was directed vertically downward and was perpendicular to the wire. A structured computational grid containing 200 nodes along the perimeter and 100 nodes on the radius was used for calculation. The computational grid was heavily clustered radially in the region of the wire.

For the vertically arranged wire, we solved the problem in an axisymmetric formulation. The computational domain represented a rectangle of height 24 cm and width 3 cm. It has been established from methodological results that such dimensions of the computational domain do not influence the calculation results. The symmetry axis was prescribed on the left-hand side of the computational domain, at whose center there was made a rectangular groove of height 8 cm and width 35 μm representing a lateral surface of the hot wire. On the walls of this groove, we prescribed a fixed heat-flux density equal to the experimental value of the heat-flux density on the wire. On the remaining boundaries of the computational domain, we specified the conditions of the absence of the heat flux. The gravity force was directed vertically downward and was coincident with the direction of the wire. Otherwise the formulation of the modeling was in complete agreement with the above case of a horizontal wire. A structured computational grid containing 600 nodes along the height and 200 nodes across the width was used for calculation. The computational grid was heavily clustered across the width in the region of the wire.

For computer-aided implementation of the above-described mathematical model, we used the developed software system "σFlow" [11–15]. Here we only mention the basic points of the numerical procedure. The difference analog of convective-diffusion equations is found using the finite-volume method for structured multiblock grids, with which the conservatism of the resulting scheme is automatically fulfilled. The upwind scheme of second order QUICKM is used for approximation of convective terms of hydrodynamic equations, and the implicit scheme of second order is employed for nonsteady terms of hydrodynamic equations. The diffusion fluxes and the source terms are approximated with the second order of accuracy. A coupling between the velocity and pressure fields is implemented using the SIMPLEC procedure on aligned grids. The Rhee–Chou approach related to the introduction of a monotonizer into the equations for a pressure correction is used to eliminate oscillations of the pressure field. The obtained system of difference equations is solved by the iterative method with a multigrid solver.

The computational algorithm was tested on a two-dimensional problem on laminar convection in the space between two coaxial cylinders. As far as the formulation is concerned, this problem is as close as possible to the hot-wire method in question for the horizontally arranged wire. The problem′s geometry is presented in Fig. 2. The radius of the external cylinder

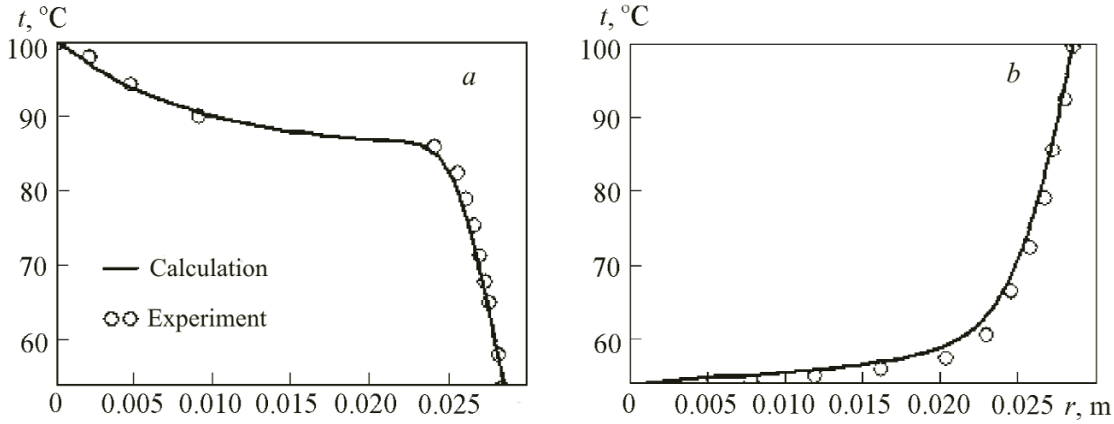

Fig. 3. Temperature distribution on the radius over (a) and under (b) the hot cylinder.

is equal to 46.3 mm, and the radius of the internal cylinder, to 17.8 mm. The walls of the internal cylinder have a temperature of 100°C, and the walls of the internal cylinder, of 54°C. The Grashof number is Gr = 49,000. For calculation, we used a multiblock computational grid consisting of 120 × 120 nodes. Experimental data were borrowed from [14].

Figure 2 compares calculated and experimental distributions of the temperature field [15] in the space between the cylinders. It is seen that qualitatively the calculated and experimental data are in good agreement. A quantitative comparison of calculation and experiment [14] is given in Fig. 3. It is seen that quantitative agreement between calculation and experiment for this problem is fairly good, too.

Next, we carried out a series of calculations of the heat transfer on the hot wire in water for different linear densities of the heat flux; the heat-flux density was varied in the range from 1 to 20 W/m. Consideration was given to the cases of vertical and horizontal arrangement of the wire. Figure 4 gives the calculated isolines of temperature at different instants of time for the case of a horizontally arranged wire at q = 13 W/m. As is seen from the calculation results, from approximately the second second after the beginning of heating, the temperature isolines deviate from concentric circles characteristic of the heat-conduction regime. In the computational domain, there begins to form a free convective flow, which becomes fully developed approximately within 5 s after the beginning of heating. Thus, at the given density of the heat flux on the hot wire, the heat-conduction regime does not exceed 2 seconds.

Figure 5 gives analogous isolines for the vertically arranged wire. For clarity of representation, the scale of Y in Fig. 5 is increased ten times compared to the scale of X. It is clear from the figures that the influence of free convection on the heat transfer begins much later than for the horizontal wire. In this case, to the heat-conduction regime there correspond isotherms in the form of symmetric elliptical curves. Such a regime on the vertical wire is observed for approximately as long as 7 s after the beginning of heating. Thereafter the elliptical curves are strongly deformed because of the influence of convection. On the wire surface, there is formed a boundary layer whose thickness increases with the wire length. Free convection becomes fully developed approximately within 10 s after the beginning of heating.

Quantitative data on the heat transfer on the wire are illustrated in Fig. 6a. The changes in the temperature $\Delta T = T_w - T_f$, where T_w is the surface-average wire temperature and T_f is the initial temperature of the fluid, on the wire are plotted versus time. For comparison with the calculation results, the plots also give the asymptotic solution (2) on which the hot-wire method is based. As is clear from the plots, because of the rejection of nonlinear terms and the influence of the heat capacity of the wire itself, this asymptotic solution disagrees with a more exact numerical solution at the beginning of the process of heat conduction. This disagreement is observed for ~0.1 s after the beginning of heating; thereafter the numerical and asymptotic solutions virtually agree, and the $\Delta T = f(\ln t)$ curves has a linear form. The calculated value of the time (0.1 s) of the beginning of the linear portion of the $\Delta T = f(\ln t)$ curve is in good agreement with the estimates obtained from the formula from [8] $\tau > \dfrac{r_w C_w \rho_w}{2\lambda_f \delta} \approx 0.18$ s, where C_w and ρ_w are the heat capacity and the density of the wire material, λ_f is the thermal conductivity of the fluid, and δ is the permissible error in determining the thermal conductivity due to the influence of the heat capacity of the heater.

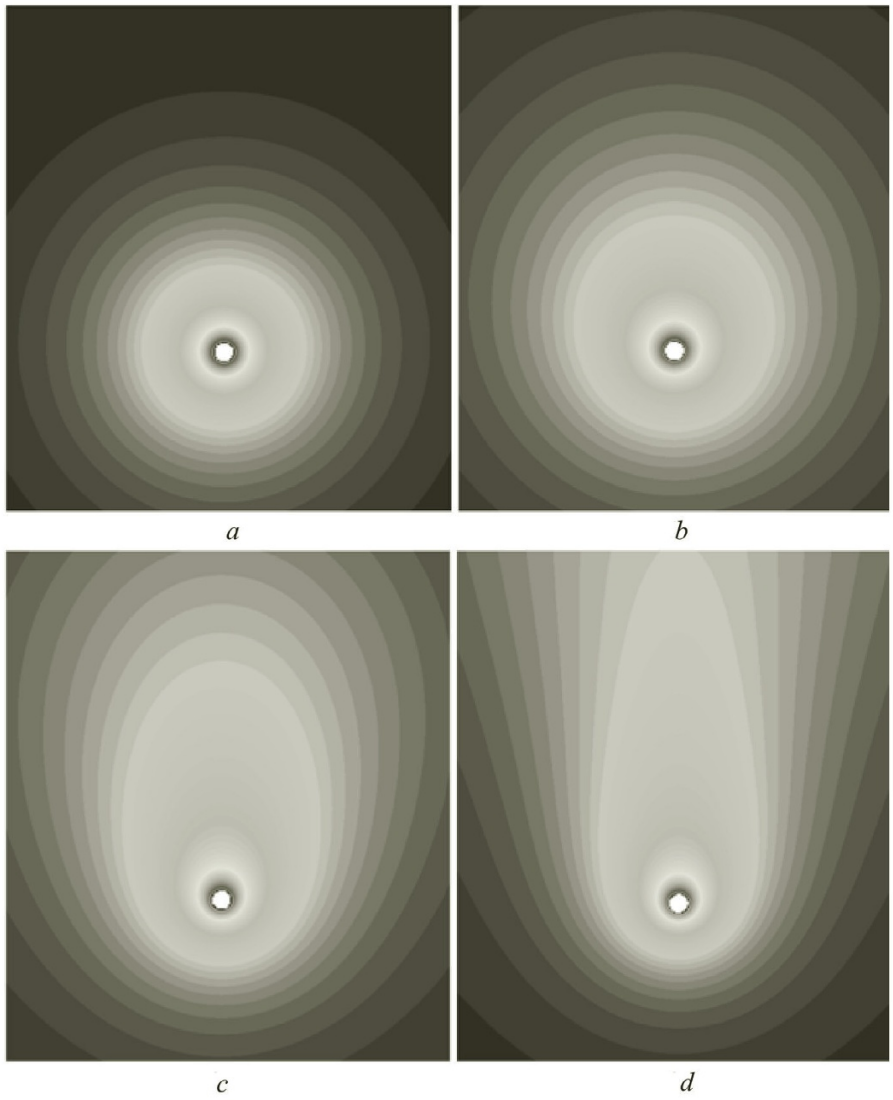

Fig. 4. Isolines of temperature at different instants of time for the horizontal arrangement of the hot wire for q = 13 W/m: a) t = 1; b) 2, c) 3, and d) 4 s.

The numerical and asymptotic solutions continue to be in agreement until a fairly intense free convective flow is formed around the wire. Depending on the orientation of the wire, this moment comes approximately within 2 s for the horizontal wire and 7 s for the vertical one. After this, the numerical and asymptotic solutions begin to strongly disagree. Thus, for our experimental parameters, the working range of the asymptotic solution used in the hot-wire method is from 0.1 to 2.2 s for the horizontal wire and from 0.1 to 7.5 s for the vertical wire. A comparison of the numerical solutions for the horizontal and vertical orientations shows that the solutions in the heat-conduction regime are in complete agreement, as they must. Differences begin once free convection has been formed. The convection begins to influence the heat transfer much earlier for the horizontal wire. Therefore, for experiments, we selected the vertical arrangement of the wire.

As far as the estimates of the time of onset of free convection available in the literature are concerned, the data differ here. We were able to find a few empirical correlations in the literature:

$$\tau > 8.3 \frac{r_w}{\alpha} \left(\frac{\mathrm{Ra} q L}{\Delta T \lambda} \right)^{-2/3} \left(\frac{L}{2 r_w} \right)^3 \text{ [16]}, \tag{4}$$

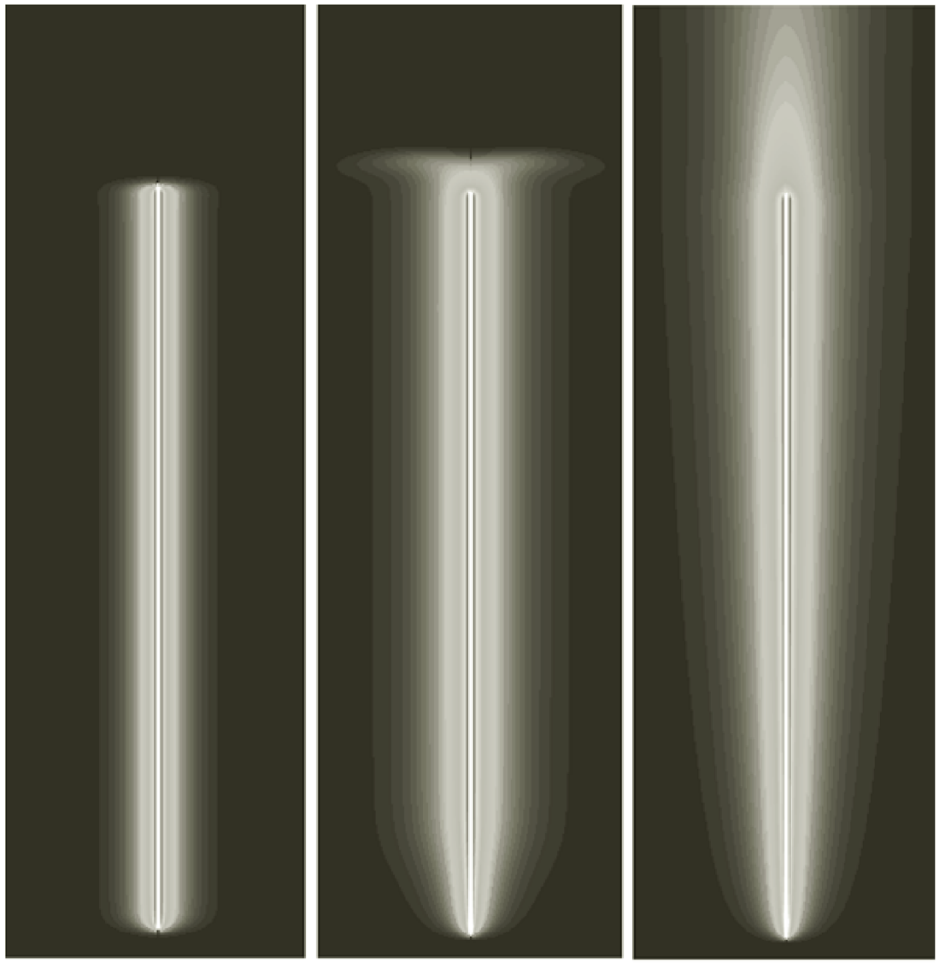

Fig. 5. Isolines of temperature at different instants of time for the vertical arrangement of the hot wire for q = 13 W/m: a) t = 5; b) 8, and c) 14 s.

$$\tau > 2.9 \frac{r_w}{\alpha} \left(\frac{\mathrm{Ra}\, q\, L}{\Delta T\, \lambda} \right)^{-2/3} \left(\frac{L}{2r_w} \right)^3 \text{ [17]}, \tag{5}$$

$$\tau > 11.92 + 49.87 \exp\left(- \frac{\mathrm{Ra}}{1.427 \cdot 10^8} \right) \text{[18]}, \tag{6}$$

where Ra is the Rayleigh number and L is the wire length. Computations from these formulas for the heat-flux density q = 13 W/m yield the following values of the time of onset of free convection: 5.8 s for formula (4), 2.1 s for (5), and 15.2 s for (6). It will be remembered that calculation at the same parameter for the vertical wire predicts a time of development of free convection of about 7.5 s, which is close to the estimates from formula (4).

Next we investigated the power of heat release on the wire. Figure 6b plots the temperature heads on the wire at a heat-flux density of 4.33 W/m (decreased three times). It can be noticed that the domain of existence of the heat-conduction regime has become much extended as far as time is concerned. For the horizontal arrangement of the wire, free convection is negligible compared to heat conduction for a period of to 3.5 s after the beginning of heating, and for the vertical arrangement, to 12 s (estimations from formula (4) yields a value of 12.3 s). This is much longer than for a heat-flux density of 13 W/m. However, at the same time, the heating of the wire surface has considerably decreased and, accordingly, the change in the

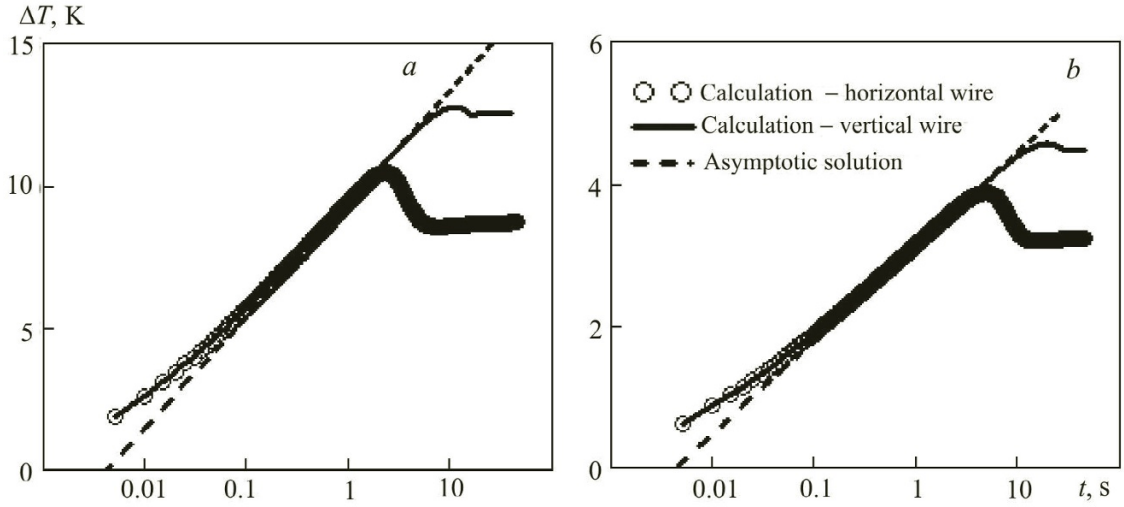

Fig. 6. Change in the temperature of the wire surface vs. time for the linear heat-flux density: a) q = 13 and b) 4.33 W/m.

electrical resistance due to the heating of the wire has decreased, too. The change in the wire′s electrical resistance is, in essence, the only instrumentally measurable quantity in the experiment. Therefore, the reduction in the heat-flux density tends to lower the sensitivity of the method. On this basis, we selected, during the experiments, values in the range from 12 to 15 W/m as the optimum linear heat-flux densities.

Thus, by numerical modeling, we have finally determined all the parameters of the experimental setup: approximate dimensions of the wire, optimum values of the heat-flux density on it, and its orientation with respect to the gravity field. We have determined ranges of applicability of the asymptotic solution used in the hot-wire method for determination of the thermal-conductivity coefficient of fluids.

Description of the Experimental Setup and Its Testing. As has been noted above, the procedure of measurement of the thermal-conductivity coefficient is based on the nonstationary (transient) hot-wire method [6–10]. The Wheatstone bridge circuit for determination of the change in the electrical resistance of the hot wire is taken as the basis of the setup. The basic electric circuit of the setup is presented in Fig. 7. We used, in the experiment, a copper wire of length 80 mm and diameter 75 μm. The wire was immersed in a glass vessel of diameter 5 cm containing 200 ml of the fluid under study. The fluid-filled vessel was heat-insulated using a foam.

The wire was one resistor of the measuring bridge R_w. Also, we used the resistors R_1 = 2 kΩ and R_3 = 1 Ω and the resistance box R_2 using which the bridge is balanced. Initially, the bridge was balanced, and the output voltage on it did not exceed 10 μV. A low voltage of 0.1 V from a GWInstek GPC-3060D laboratory power supply was fed during a short period of time to balance the measuring system.

Therefore, we fed measuring voltage to the circuit and recorded the change in the voltage of disbalance of the bridge circuit with time. Measurements of the voltage were carried out using a GWInstek GDM-78261 precision voltmeter with a step of 10 ms, and measurements of the temperature of the fluid under study, using Chromel-Copel thermocouples connected to a TPM138 meter.

The obtained data are processed according to the following formulas.

The initial resistance of the wire is found from the condition of balance of the bridge circuit: $\frac{R_1}{R_2} = \frac{R_{w0}}{R_3}$. Consequently, the resistance of the wire is equal to $R_{w0} = \frac{R_1}{R_2} R_3$. The change in the wire′s resistance is determined as

$$R_{wt} = \frac{R_3 \left[R_1 + (R_1 + R_2) \frac{V_{out}}{V_{in}} \right]}{\left[R_2 - (R_1 + R_2) \frac{V_{out}}{V_{in}} \right]},$$

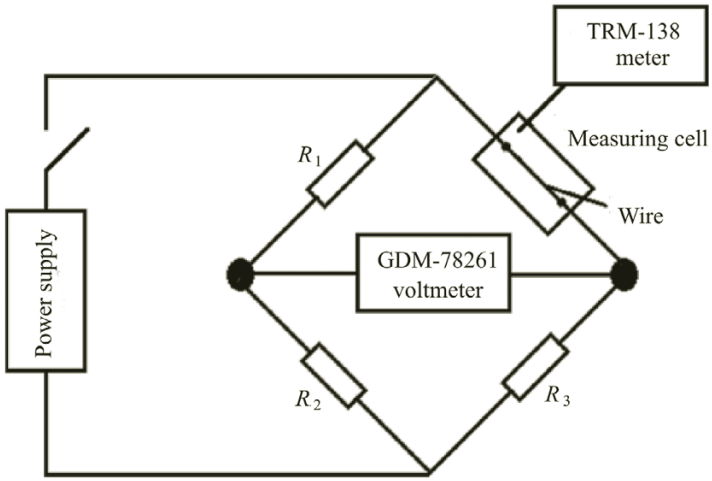

Fig. 7. Electric circuit of the setup.

where $V_{\rm m}$ is the input voltage of the bridge and $V_{\rm out}$ is the voltage of the disbalanced bridge.

Taking into account the temperature dependence of the electrical resistance of the copper, we can determine the change in the wire temperature

$$\Delta T = \frac{1}{\alpha}\,\frac{R_{\rm wt2} - R_{\rm wt1}}{R_{\rm w0}} = \frac{\Delta R_{\rm w}}{\alpha R_{\rm w0}}\,.$$

To determine the temperature coefficient of electrical resistance α, we performed in advance a special series of measurements of the resistance of the copper wire in use at different temperatures. It has been established by these measurements that α = 0.000383 1/K.

The voltage drop on the wire is determined from the formula $V_{R\rm w} = \dfrac{V_{\rm in} R_{\rm wt}}{R_{\rm wt} + R_3}$; then the linear heat-flux density on the wire is equal to $q = \dfrac{(V_{R\rm w})^2}{L_{\rm w} R_{\rm wt}}$, where $L_{\rm w}$ is the wire length.

Finally, from the theory given above, the thermal-conductivity coefficient of the fluid is determined as follows:

$$\lambda = \frac{q}{4\pi H} = \alpha R_{\rm w0}\,\frac{q}{4\pi}\,\frac{1}{G}\,. \tag{7}$$

Let us evaluate the relative error of measurement of the thermal-conductivity coefficient, which is made up of the errors of measurement of the heat-flux density q, the temperature coefficient of electrical resistance α, the initial resistance of the wire R_0, and the slope $\Delta R \sim \ln t$ — G:

$$\delta_\lambda = \sqrt{\left(\frac{\partial\lambda}{\partial q}\,\delta_q\right)^2 + \left(\frac{\partial\lambda}{\partial\alpha}\,\delta_\alpha\right)^2 + \left(\frac{\partial\lambda}{\partial R_{\rm w0}}\,\delta_{R\rm w0}\right)^2 + \left(\frac{\partial\lambda}{\partial G}\,\delta_G\right)^2}\,.$$

The relative error of measurement of the heat-flux density is in turn determined as

$$\delta_q = \sqrt{\left(\frac{\partial q}{\partial V_{R\rm w}}\,\delta_{VR\rm w}\right)^2 + \left(\frac{\partial q}{\partial R_{\rm wt}}\,\delta_{R\rm wt}\right)^2 + \left(\frac{\partial q}{\partial L_{\rm w}}\,\delta_{L\rm w}\right)^2}\,,$$

where $\delta_{VR\rm w}$ is the error of measurement of the voltage drop on the wire:

$$\delta_{VR\rm w} = \sqrt{\left(\frac{\partial V_{R\rm w}}{\partial V_{\rm in}}\,\delta_{V\rm in}\right)^2 + \left(\frac{\partial V_{R\rm w}}{\partial R_{\rm wt}}\,\delta_{R\rm wt}\right)^2 + \left(\frac{\partial V_{R\rm w}}{\partial R_3}\,\delta_{R3}\right)^2}\,,$$

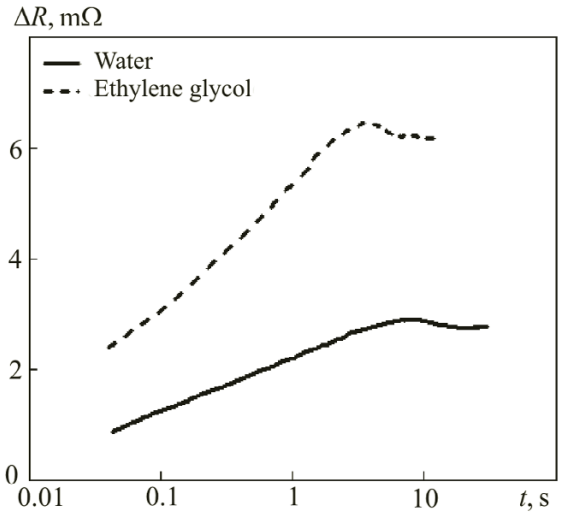

Fig. 8. Change in the electrical resistance of the wire in the process of its heating for a linear heat-flux density of 14 W/m.

TABLE 1. Comparison of the Measured Values of the Thermal-Conductivity Coefficient of Water at a Temperature of 25°C and the Experimental Data

Experiment number	λ_m, W/(m·K)	λ_{ref} [19], W/(m·K)	Deviation, %
1	0.610		0.5
2	0.608		0.2
3	0.619	0.607	2.0
4	0.612		0.8
5	0.616		1.4

δ_{Rwt} is the error of measurement of the wire's resistance:

$$\delta_{Rwt} = \sqrt{\left(\frac{\partial R_{wt}}{\partial R_1}\,\delta_{R_1}\right)^2 + \left(\frac{\partial R_{wt}}{\partial R_2}\,\delta_{R_2}\right)^2 + \left(\frac{\partial R_{wt}}{\partial R_3}\,\delta_{R_3}\right)^2 + \left(\frac{\partial R_{wt}}{\partial V_{out}}\,\delta_{V\text{out}}\right)^2 + \left(\frac{\partial R_{wt}}{\partial V_{in}}\,\delta_{V\text{in}}\right)^2},$$

$\delta_{Lw} \approx 0.6\%$ of the error of measurement of the wire length, and δ_{Rw0} is the error of measurement of the wire's initial resistance:

$$\delta_{Rw0} = \sqrt{\left(\frac{\partial R_{w0}}{\partial R_1}\,\delta_{R1}\right)^2 + \left(\frac{\partial R_{w0}}{\partial R_2}\,\delta_{R2}\right)^2 + \left(\frac{\partial R_{w0}}{\partial R_3}\,\delta_{R3}\right)^2}.$$

The error of predetermining α amounts to 1.2%. The computations show that the relative error of determination of the slope G by the least-squares method amounts to about 0.5%. The errors of determination of the remaining quantities are equal to $\delta_{V_{in}} = 0.008\%$, $\delta_{V_{out}} = 0.02\%$, $\delta_{R3} = 0.41\%$, $\delta_{R1} = 0.01\%$, and $\delta_{R2} = 0.02\%$. Thus, the final relative error of measurement of the thermal-conductivity coefficient of the fluid δ_λ by this procedure amounts to about 3%.

To test the experimental procedure, we carried out a series of measurements on pure index liquids (water and ethylene glycol). Typical changes in the electrical resistance of the wire with time in its heating in water and ethylene glycol are given in Fig. 8. Using these data, we can obtain, from formula (7), the values of the thermal-conductivity coefficient of the liquids. The thermal-conductivity coefficient was measured five times for each liquid. The final values were obtained by averaging over these five measurements. All the measurements were carried out at a room temperature of 25°C.

TABLE 2. Comparison of the Measured Values of the Thermal-Conductivity Coefficient of Ethylene Glycol at a Temperature of 25°C and the Experimental Data

Experiment number	λ_m, W/(m·K)	λ_{ref} [20], W/(m·K)	Deviation, %
1	0.260		2.3
2	0.261		2.7
3	0.251	0.254	1.2
4	0.259		1.9
5	0.262		3.1

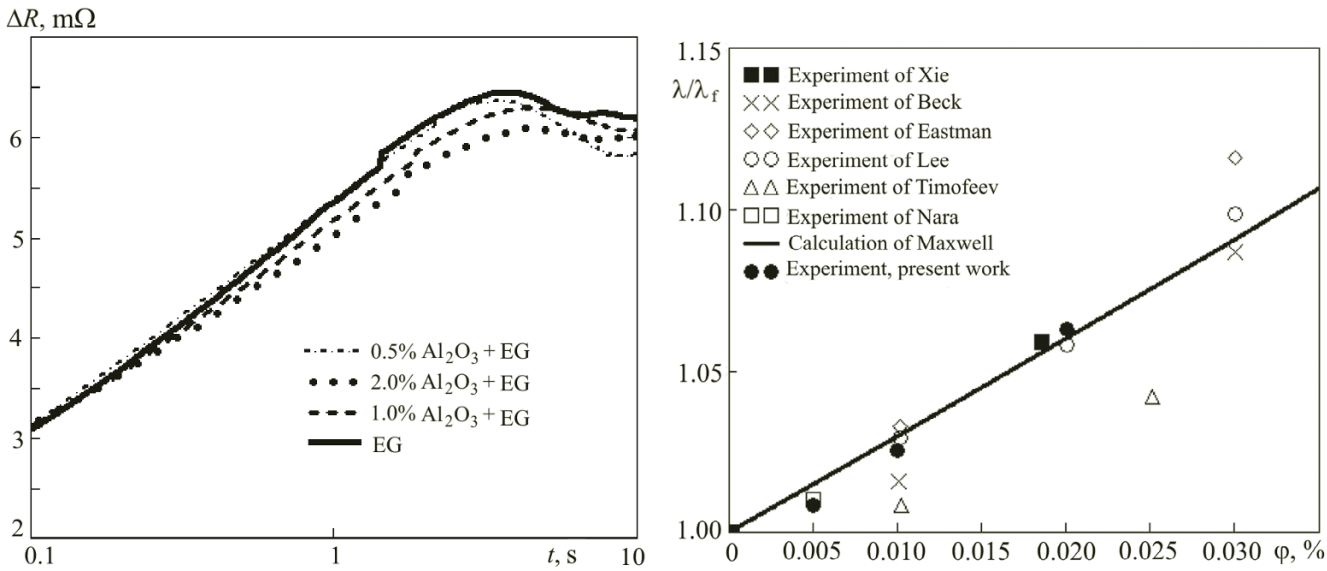

Fig. 9. Electrical resistance of the wire in the process of its heating vs. concentration of nanoparticles in ethylene glycol at a linear heat-flux density of 14 W/m.

Fig. 10. Change in the measured thermal-conductivity coefficient vs. concentration of alumina nanoparticles in ethylene glycol at a temperature of 25°C.

Tables 1 and 2 list the obtained results of measurements of the thermal-conductivity coefficient of water and ethylene glycol and compare them to the reference data. A fairly good agreement is seen to be obtained between the measured thermal-conductivity coefficient and the literature data [19, 20]. The maximum disagreement amounts to 1.4% for water and to 3.1% for ethylene glycol, which is within the methodological error.

Measurement of the Thermal-Conductivity Coefficient of a Nanofluid. Using this experimental procedure we measured the thermal-conductivity coefficient of a nanofluid based on alumina nanoparticles. The carrier liquid was ethylene glycol. The volume concentration was varied from 0.5 to 2%. A standard two-step process was used to prepare the nanofluid. On adding the necessary amount of a nanopowder to water, we placed the vessel with a nanofluid in a UZDN-A ultrasonic disperser for half an hour to destroy conglomerates of nanoparticles. The alumina nanoparticles were purchased from Plazmoterm Company (Moscow). According to the data of an x-ray phase analysis, the specific surface of the powder was 30 m^2/g, which corresponded to an average nanoparticle size of 50 nm. All the measurements were carried out at a room temperature of 25°C.

The time dependence of the change in the electrical resistance of the wire in its heating in the nanofluid with different volume concentrations of the alumina particles is shown in Fig. 9. It is seen that the slope of the nanoparticle concentration to

the time axis decreases. This is due to the growth in the thermal-conductivity coefficient of the medium with the concentration of the nanoparticles.

The measured effective thermal-conductivity coefficient is plotted versus the concentrations of the alumina nanoparticles in ethylene glycol in Fig. 10. The plot gives the values of the ratio of the thermal-conductivity coefficient of the nanofluid to the thermal-conductivity coefficient of the basic liquid. Measurement results obtained by other authors [21–26] are given for comparison. As is seen from the plots, our measurements agree well with the results of most of the foreign experimental data. The disagreement of experimental thermal-conductivity data obtained by different authors reflects, on the whole, the current status of research in the field of heat transfer of nanofluids: there is no reproducibility of results, and experiments often contradict one another, and this despite the fact that an alumina-based nanofluid is the most studied nanofluid. The situation is much worse for other nanofluids.

For comparison with experiments, the plots also give the thermal-conductivity coefficient values obtained from the Maxwell correlation [27]

$$\frac{\lambda}{\lambda_f} = \frac{\lambda_p + 2\lambda_f + 2\varphi\left(\lambda_p - \lambda_f\right)}{\lambda_p + 2\lambda_f - \varphi\left(\lambda_p - \lambda_f\right)},$$

where λ_p and λ_f are the thermal-conductivity coefficients of the particles′ material and of the basic liquid and φ is the volume concentration of the nanoparticles. This formula is widely used to determine the thermal-conductivity coefficient of a suspension of solid particles in liquids which are nanofluids. As is seen, for a nanofluid based on alumina and ethylene glycol, experimental values of the thermal-conductivity coefficient in the investigated range of concentration are satisfactorily described by the Maxwell correlation. Probably, this is due to the fact that relatively large (50 nm) alumina particles were used for preparation of the nanofluid.

Conclusions. As a result of the work carried out, the authors have created and tested an experimental setup making it possible to determine, with an acceptable degree of accuracy, the values of the thermal-conductivity coefficient of fluid media on the basis of the hot-wire method. A two-dimensional mathematical model of heat transfer with allowance for free convection has been constructed to describe processes occurring on the wire in its unsteady heating. Using this model we have finally determined the parameters of the experimental setup and the ranges of correct applicability of the asymptotic solution used in the hot-wire method for determination of the thermal-conductivity coefficient of fluids. The experimental procedure was tested during the measurement of the thermal-conductivity coefficient of water and ethylene glycol. The disagreement between the measurements and the reference data did not exceed ~3%. The authors have shown the applicability of the procedure to measurement of the thermal conductivity of nanofluids: they measured the thermal conductivity of a nanofluid based on alumina-oxide nanoparticles. The carrier liquid was ethylene glycol. The measurement results have been compared to the data of other authors and the Maxwell correlation. Good agreement of the results has been obtained. Noteworthy is another important circumstance. In analyzing experimental results obtained by the hot-wire method, some researchers voice concerns that nanoparticles are deposited on the wire surface in the process of measurements of the thermal-conductivity coefficient of a nanofluid. This results in the distortion of the measurements with time. These concerns were refuted by us experimentally. After multiple measurements in nanofluids with different concentrations, we carried out measurements again on pure fluids. No deviations of the measured thermal-conductivity coefficient from the values obtained earlier were established. Thus, we will further use this procedure for systematic investigations of the thermal-conductivity coefficient of various nanofluids.

This work was carried out with partial financial support from the Russian Scientific Foundation (agreement No. 14-19-00312).

NOTATION

a, thermal-diffusivity coefficient, m2/s; C_p and C_f, specific heats of the particles′ material and of the basic fluid respectively, J/(kg·K); g, free-fall acceleration, m/s^2; G, angle of slope of $\Delta R \sim \ln t$; Gr, Grashof number; H, angle of slope of $\Delta T \sim \ln t$; h, enthalpy, J; L, length, m; p, pressure, Pa; q, heat-flux density per unit length, W/m; R, resistance, Ω; R_{w0}, resistance of the wire at the balance of the bridge, Ω; R_{wt}, resistance of the wire at the instant of time t, Ω; ΔR, change in the resistance, Ω; R_1, R_2, and R_3, resistances of the high-impedance resistor, of the resistance box, and of the low-impedance resistor in the Wheatstone bridge respectively, Ω; r, radius, m; r_w, radius of the wire, m; T, temperature, ^oC; T_0, room temperature, ^oC; **T**, viscous-stress tensor; ΔT, change in the wire temperature, ^oC; T_f, initial temperature of the fluid, ^oC; T_w, surface-average

temperature of the wire, ^{o}C; t, time, s; **v**, velocity vector; V_{in}, voltage on the wire, V; V_{out}, voltage of the disbalanced bridge, W; V_{Rw}, voltage drop on the wire, V; α, coefficient of temperature resistance, 1/^{o}C; β, coefficient of thermal expansion of the fluid, 1/m^3; λ, thermal-conductivity coefficient, W/(m·K); λ_p and λ_f, thermal-conductivity coefficients of the particles′ material and the basic fluid respectively, W/(m·K); ν, kinematic viscosity, m^2/s; ρ, density of the fluid, kg/m^3; ρ_0, density of the fluid at room temperature, kg/m^3; φ, volume concentration of nanoparticles, %.

REFERENCES

1. A. S. Ahuja, Augmentation of heat transport in laminar flow of polystyrene suspensions. II. Analysis of the data, *J. Appl. Phys.*, **46**, 3417–3425(1975)
2. S. Choi, Enhancing thermal conductivity of fluids with nanoparticles, in: D. A. Siginer and H. P. Wang (Eds.), *Developments and Applications of Non-Newtonian Flows*, *ASME*, New York, **231**, 99–105 (1995).
3. V. I. Terekhov, S. V. Kalinina, and V. V. Lemanov, Mechanism of heat transfer in nanofluids: current status of the problem. Part 2. Convective heat transfer, *Teplofiz. Aéromekh*., No. 2, 173–188 (2010).
4. L. Godson, B. Raja, D. Mohan Lal, S. Wongwises, Enhancement of heat transfer using nanofluids — an overview, *Renew. Sustain. Energy Rev.*, **14**, 629–641 (2010).
5. B. Pak and Y. I. Cho, Hydrodynamic and heat transfer study of dispersed fluids with submicron metallic oxide particle, *Exp. Heat Transfer*, **11**, 151–170 (1998).
6. A. Schleiermacher, *Ann. Phys. Chem.*, **34**, No. 6, 346 (1888).
7. A. G. Shashkov, G. M. Volokhov, T. N. Abramenko, and V. P. Kozlov (A. V. Luikov Ed.), *Methods of Determination of Thermal Conductivity and Thermal Diffusivity* [in Russian], Énergiya, Moscow (1973).
8. E. S. Platunov, I. V. Baranov, S. E. Buravoi, and V. V. Kurepin (E. S. Platunov Ed.), *Thermophysical Measurements: a Manual* [in Russian], SPbGUN and PT, St. Petersburg (2010).
9. R. G. Richard and I. R. Shankland, A transient hot-wire method for measuring the thermal conductivity of gases and liquids. *Int. J. Thermophys*., **10**, No. 3, 673–686 (1989).
10. M. Kostic and Kalyan C. Simham, Computerized, transient hot-wire thermal conductivity (HWTC) apparatus for nano-fluids, in: *Proc. 6th WSEAS Int. Conf. on Heat and Mass Transfer (HMT'09)*, 71–78 (2009).
11. A. A. Gavrilov, A. V. Minakov, A. A. Dekterev, and V. Ya. Rudyak, Numerical algorithm for modeling of laminar flows in an annular channel with eccentricity, *Sib. Zh. Ind. Mat*., **13**, No. 4, 3–14 (2010).
12. V. Ya. Rudyak, A. V. Minakov, A. A. Gavrilov, and A. A. Dekterev, Application of new numerical algorithm for solving the Navier–Stokes equations for modelling the work of a viscometer of the physical pendulum type, *Thermophys. Aeromech.*, **15**, No. 2, 333–345 (2008).
13. V. Ya. Rudyak, A. V. Minakov, A. A. Gavrilov, and A. A. Dekterev, Modelling of flows in micromixers, *Thermophys. Aeromech*., **17**, No. 4, 565–576 (2010).
14. T. H. Kuehn and R. J. Goldstein, An experimental and theoretical study of natural convection heat transfer in concentric and eccentric horizontal cylindrical annuli, *ASME J. Heat Transf*., **100**, 635–640 (1978).
15. M. Van Dyke, *Album of Liquid and Gas Flows* [Russian translation], Mir, Moscow (1986).
16. X. Zhang, S. Fujiwara, Z. Qi, and M. Fujii, Natural convection effect on transient short-hot-wire method, *J. Jpn. Soc. Microgravity Appl.*, **16**, No. 2, 129–135 (1999).
17. Huaqing Xie, Hua Gu, Motoo Fujii, Xing Zhang, Short hot wire technique for measuring thermal conductivity and thermal diffusivity of various materials, *Meas. Sci. Technol*., **17**, 208–214 (2006).
18. Seung-Hyun Lee, Hyun Jin Kim, Seok Pil Jang, Onset of natural convection in transient hot-wire device for measuring thermal conductivity of nanofluids, *Trans. Korean Soc. Mech. Eng.*, **35**, 279–285 (2011).
19. A. I. Volkov and I. M. Zharskii, *Great Chemical Reference Book* [in Russian], Sovremennaya Shkola, Minsk (2005).
20. I. S. Grigor′eva and E. Z. Meilikhova, *Physical Quantities, a Reference Book* [in Russian], Énergoatomizdat, Moscow (1991).
21. H. Xie, J. Wang, T. Xi, Y. Liu, and F. Ai, Thermal conductivity enhancement of suspensions containing nanosized alumina particles, *J. Appl. Phys.*, **91**, 4568–4572 (2002).
22. M. P. Beck, T. Sun, and A. S. Teja, The thermal conductivity of alumina nanoparticles dispersed in ethylene glycol, *Fluid Phase Equilibria*, **260**, No. 2, 275–278 (2007).
23. J. A. Eastman, S. U. S. Choi, S. Li, W. Yu, and L. J. Thompson, Anomalously increased effective thermal conductivities of ethylene glycol-based nanofluids containing copper nanoparticles, *Appl. Phys. Lett.*, **78**, 718–720 (2001).

24. S. Lee, S. U. S. Choi, S. Li, and J. A. Eastman, Measuring thermal conductivity of fluids containing oxide nanoparticles, *ASME J. Heat Transf.*, **121**, 280–289 (1999).
25. E. V. Timofeeva, A. N. Gavrilov, J. M. McCloskey, and Y. V. Tolmachev, Thermal conductivity and particle agglomeration in alumina nanofluids: experiment and theory, *Phys. Rev.*, E76:061203 (2007).
26. S. Nara, P. Bhattacharya, P. Vijayan, W. Lai, P. Phelan, R. Prasher, D. Song, and J. Wang, *2005 ASME International Mechanical Engineering Congress and Exposition,* Orlando, Florida, USA, 80524 (2005).
27. J. C. Maxwell, *A Treatise on Electricity and Magnetism*, 2nd edn., Vol. 1, Clarendon Press, Oxford (1881).